Check for updates

Adsorption of reactive dye from aqueous solution and synthetic dye bath wastewater by *Eucalyptus* bark/magnetite composite

Behzat Balci and Fatma Elcin Erkurt

ABSTRACT

In the present study, *Eucalyptus camaldulensis* bark/magnetite composite (EBMC) was used for a potential application as a low-cost adsorbent for the removal of Reactive Black 5 (RB5). The adsorption experiments were performed with aqueous solution (RB5 + distilled water) and synthetic dye bath wastewater (SDBW) in order to investigate the potential application of EBMC in the textile industry. The effects of the various parameters, the initial dye concentration, the temperature, the pH, and the EBMC dosage on the adsorption were investigated. It was found that the adsorption capacity of EBMC increases by increasing the RB5 concentration and temperature and by decreasing the dosage of EBMC. 0.8 g EBMC was found to be sufficient for the removal of 250 mg/L RB5 from 150 mL SDBW with ~85% removal efficiency. The Koble–Corrigan isotherm model described the adsorption process more effectively ($R^2 = 0.997$) than the Langmuir, Freundlich, the Dubinin–Radushkevich and the Jovanovic isotherm models. The Langmuir isotherm predicted a 370.7 mg/g maximum adsorption capacity. The thermodynamic analysis showed that the adsorption of RB5 onto the EBMC was an endothermic process. The multiple linear regression analysis was used in order to determine the cumulative effects of independent variables on the adsorption capacity.

Key words | *Eucalyptus camaldulensis*, magnetite, Reactive Black 5

Behzat Balci (corresponding author)
Fatma Elcin Erkurt
Cukurova University Department of Environmental Engineering,
Balcali/Saricam,
Adana 01136,
Turkey
E-mail: *behzatbalci@gmail.com*

INTRODUCTION

Dyes usually have a synthetic origin and complex aromatic structures. These synthetic dyes are widely used in the textile, food, pharmaceutical, tanning, cosmetics, and electroplating industries (Saban Tanyildizi 2011). These industrial processes can discharge wastewaters containing dye into water systems (Mohan *et al.* 2002). The presence of dyes in water systems reduces the light penetration into the deeper layers, lowers the gas solubility, diminishes the photosynthetic activity and, at the same time, the water quality deteriorates (Myslak & Bolt 1988; Kumar *et al.* 2012). The methods generally used for treating dye-containing wastewaters are membrane filtration, coagulation-flocculation (Crawford & Gretlyn 1990), and adsorption (Wong *et al.* 2004). Adsorption is a widely used and effective physical method for the treatment of colored wastewater. Adsorption systems have gained prominence as treatment processes that ensure good quality effluents that are low in concentrations of dissolved organic compounds such as dyes (Walker & Weatherley 1997). Magnetic particle technology has received considerable attention in recent years as a way to help solve environmental problems (Luiz *et al.* 2004). The magnetite (Fe_3O_4) nanoparticles can be used as a surface coating material in adsorption processes to enhance the surface properties of the adsorbents. These nano-adsorbents have attracted substantial interest in adsorption studies because of their high surface area and highly active surface sites (Nethaji *et al.* 2013). Dye adsorption studies are usually performed with aqueous solution (dye + distilled water) (Malik 2003; Elsa *et al.* 2008; Nevine 2008; Suhong *et al.* 2010; Taimur *et al.* 2010; Wang 2012; Mohammad *et al.* 2014; Kouassi *et al.* 2015; Gabriela *et al.* 2016). Undoubtedly, the adsorption studies performed with distilled water are important in order to understand the specific sorption interactions between the adsorbents and the dye molecules. However, textile dye bath wastewater may contain more impurities, such as alkalinity, acidity, NH_4-N, Cl^- ions, suspended

doi: 10.2166/wst.2016.323

Downloaded from https://iwaponline.com/wst/article-pdf/74/6/1386/458808/wst074061386.pdf
by guest

solids, and oil/grease (Ipek *et al.* 2006; Ilda *et al.* 2012). Therefore, low dye removal efficiencies may occur due to the competitive sorption between the dye molecules and these impurities in the potential application of the adsorbents for the removal of dyes from textile wastewater.

The main objective of this study is to investigate the use of *Eucalyptus camaldulensis* bark/magnetite composite (EBMC) as a novel low-cost adsorbent for the removal of Reactive Black 5 (RB5) from aqueous solution and synthetic dye bath wastewater (SDBW). The *E. camaldulensis* barks were selected as a low-cost adsorbent due to their renewable character, wide availability and accessibility.

MATERIAL AND METHODS

Preparation of adsorbent

In the southern region of Turkey, *E. camaldulensis* is a common species. It is native to Australia. The large evergreen tree *E. camaldulensis* is 24–40 m high, and its stout trunk is often short and crooked. It is 2 m in diameter and the crown is open, wide and spreads irregularly. Their bark is smooth, white, gray, or buff (Little 1983). According to Yadav *et al.* (2002), the chemical composition of the Eucalyptus barks is generally organic and percentages in a dry weight basis (w/w) of the composition of bark is 37.4 cellulose, 19.2 hemicellulose, 5.5 free sugars, 62.2 total carbohydrates, 28.0 lignin, 4.9 ash, 1.1 total nitrogen, 15.5 water extractables, 7.2 alcohol extractables, and 93.2 total organic matter. The barks of *E. camaldulensis* were collected from the Balcali campus of the University of Cukurova (Adana, Turkey). Upon collection, the barks were crushed and sieved to a median value of a 0.125 mm particle size, and then washed with distilled water in order to remove any impurities.

The EBMC was prepared with the co-precipitation technique. 5 g *Eucalyptus* bark was added into a 2,000 mL solution containing 5.82 g $FeCl_3{\cdot}6H_2O$ and 3 g $FeSO_4.7H_2O$ stirred at 70 °C for 1.5 h under N_2 atmosphere. Then a NaOH solution (5 mol/L) was added dropwise to the precipitate iron oxide. The mixtures were aged at 70 °C for 3 h, then washed with distilled water, and dried at 60 °C for 24 h.

Dye and measurement

The azoic structure dye RB5 was obtained from the local textile industry in Turkey. The RB5 concentration of the supernatant was estimated by measuring the absorbance at the maximum wavelengths (597 nm) and computing the concentration from the calibration curve. The calibration curve was prepared with a Perkin Elmer Lambda 35 UV/VIS spectrophotometer. The concentrations of the calibration curves ranged between 2.5 and 25 mg/L. The dye concentrations over 25 mg/L were analyzed by the dilution of the samples. The molecule structure of the RB5 is given in Figure 1.

Statistical analysis

The statistical evaluations were performed using SPSS Statistics 20.0 with a confidence interval of 95% ($p \leq 0.05$). The experiments were repeated three times, and the average value was used for the calculations. Also, the multiple linear regression (MLR) analysis was used in order to determine the cumulative effects of the independent variables such as the time, the pH, the temperature, the RB5 concentration, and the EBMC dosage on the adsorption capacity at the equilibrium (q_e) as a dependent variable.

Mathematical expression of MLR can be represented as:

$$Y = a_0 + a_i X_i + a_2 X_2 \cdots + a_n X_n + \varepsilon \quad (1)$$

Y is the dependent (predicted) variable, a_i (i = 0,. . .,n) are the regression coefficients, X_i (i = 1,. . .,n) are the independent variables (predictors) and ε shows the stochastic error of the regression (Utkan *et al.* 2011). In this study, the MLR analysis was performed in order to examine the cumulative effects of the independent variables such as the contact time, the pH, the temperature, the BPA concentration, and the adsorbent dosage on the equilibrium adsorption capacity of the EBMC as a dependent variable. SPSS statistics 20.0 was used for the MLR analyses.

Adsorption tests

The batch experiments were performed for the adsorption of the RB5 with EBMC. 500 mL Erlenmeyer flasks were used,

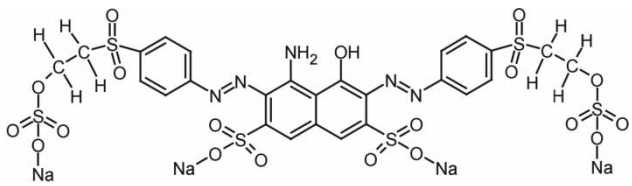


Figure 1 | The molecule structure of RB5.

Downloaded from https://iwaponline.com/wst/article-pdf/74/6/1386/458808/wst074061386.pdf
by guest

each containing 150 mL RB5 solution with different concentrations and the desired weight of EBMC. The flasks were stirred at 250 rpm in a temperature-controlled orbital shaker. The effect of the initial dye concentration (75, 100, 150, 200 and 250 mg/L), EBMC dosage (0.1, 0.2, 0.4, 0.6 and 0.8 g), temperature (15, 20, 25, 30, 35, 40, 45, 50 and 50 °C), and pH (2, 3, 4, 5, 6, 7, 8, 9 and 10) on the adsorption were studied. The adsorption tests were performed with distilled water and SDBW. The composition of the SDBW without the RB5 was (mg/L); NH_4-N 6, oil/grease 160, chloride 18000 (Ipek *et al.* 2006; Ilda *et al.* 2012). The samples were withdrawn at certain time intervals during the adsorption test, centrifuged for 5 min at 4,000 rpm, and a supernatant was used to determine the residual dye concentration. The data were used to calculate the adsorption capacity at different times, q_t, of EBMC.

The amount of the RB5 adsorbed into the EBMC at different times (q_t) was calculated from Equation (2):

$$q_t = \frac{(C_0 - C_e)V}{W} \tag{2}$$

and dye removal efficiency was calculated as:

$$\text{Dye Removal Efficiency (\%)} = \frac{C_t - C_0}{C_0} \times 100 \tag{3}$$

C_0 = Initial RB5 concentration, mg/L,
C_e = RB5 concentration at equilibrium time, mg/L,
C_t = RB5 concentration at time (t), mg/L,
V = Volume of the aqueous phase, L,
W = The amount of EBMC, g.

Equilibrium isotherms

The adsorption isotherms indicate the distribution of the adsorption molecules between the liquid phase and the solid phase at the equilibrium point. The analysis for fitting the isotherm to the adsorption isotherm models is a major stage for finding the best model to be used for the design of the adsorption systems (Senthil Kumar *et al.* 2010). The isotherm parameters were calculated according to the non-linear regression method due to the inherent bias resulting from the linearization of the adsorption equations. Non-linear regression ensures a mathematically sensitive method for calculating the parameters of the isotherms by using the original form of the isotherm equation (Chan *et al.* 2012). The minimization procedure is performed to solve the adsorption isotherm equations by maximizing the correlation coefficient between the experimental data points and the theoretical model predictions with the solver add-in function of Microsoft Excel (Wong *et al.* 2004). The criteria for the selection of the best isotherm model are essentially based on the correlation coefficient and the average percentage errors (APEs). The correlation coefficient shows the fit between the experimental data and isotherm model, while the APEs indicate the fit between the experimental data and the calculated data used for plotting the isotherm curves (Subramanyam & Ashutosh 2012). The equation of APE can be written as:

$$APE(\%) = \frac{\sum_{i=1}^{N} \left| ((q_e)_{\exp} - (q_e)_{cal})/(q_e)_{\exp} \right|}{N} \times 100 \tag{4}$$

where q_e is the amount of the adsorbate adsorbed per unit mass of the adsorbent (mg/g) at equilibrium, N is the amount of experimental data.

Langmuir isotherm

This model assumes monolayer adsorption onto the homogenous adsorbent surface. The Langmuir isotherm can be represented as:

$$q_e = \frac{q_{\max} K_L C_e}{1 + K_L C_e} \tag{5}$$

where q_e is the amount of adsorbate adsorbed per unit mass of adsorbent (mg/g) at the equilibrium, C_e is the equilibrium concentration of the adsorbate (mg/L), q_{max} is the maximum adsorption capacity (mg/g) and K_L is the Langmuir constant related to the adsorption rate (L/mg) (Langmuir 1918).

Freundlich isotherm

Freundlich improved an empirical equation applied to define the heterogeneous adsorption processes (Freundlich 1906). The Freundlich isotherm equation can be represented as:

$$q_e = K_F C_e^{1/n} \tag{6}$$

K_F is the Freundlich isotherm constant (L/mg). 1/n represents the intensity of the surface heterogeneity and ranges

Downloaded from https://iwaponline.com/wst/article-pdf/74/6/1386/458808/wst074061386.pdf
by guest

between 0 and 1. A value of 1/n closer to zero indicates the high intensity of the surface heterogeneity (Weber & Chakkravorti 1974).

Dubinin–Radushkevich isotherm

Dubinin and Radushkevich (D-R) assume the adsorbed possesses a multilayer character (Dabrowski 2001). The equation of the D-R isotherm is given by the following equation:

$$q_e = q_{\max} \exp\left(-B_D \varepsilon^2\right) \tag{7}$$

$$\varepsilon = RT \ln\left(1 + \frac{1}{C_e}\right) \tag{8}$$

where q_{max} is the maximum adsorption capacity (mg/g), B_D (mol^2k/J^2) is D-R constant, ε is the Polanyi constant, R is the gas constant (8.31 J/mol K), and T is the absolute temperature (Bennani *et al.* 2009).

Jovanovic isotherm

The Jovanovic model was derived for an adsorption on a homogeneous solid surface, considering the phenomenon non-specific, without lateral interactions, and covering the surface with a monolayer of the solute. The equation of the Jovanovic isotherm is given as:

$$q_e = q_{\max}\left(1 - e^{(K_j C_e)}\right) \tag{9}$$

where q_{max} is the maximum adsorption capacity (mg/g) and Kj is the model constant (Rafael *et al.* 2013).

Koble–Corrigan isotherm

The Koble–Corrigan isotherm is a three-parameter equation, incorporated with both the Langmuir and Freundlich isotherm.

$$q_e = \frac{aC_e^n}{1 + bC_e^n} \tag{10}$$

where a and b are the isotherm parameters and n is the model exponent (Foo & Hameed 2010).

RESULTS AND DISCUSSION

Effect of the contact time on adsorption

The correct representation of the dynamic adsorptive separation of the RB5 from the aquatic phase onto EBMC depends on an accurate understanding of the equilibrium separation between the RB5 solution and the EBMC (Allen *et al.* 2003). The equilibrium time gives the optimum time for the removal of the RB5 from the aqueous solutions. The contact time experiments were performed for the EBMC with distilled water and SDBW. The effect of the contact times on the adsorption capacity of the EBMC (0.1 g) for 250 mg/L RB5 at 20 °C and pH = 7 is shown in Figure 2. 70 min is necessary to reach equilibrium for the RB5 adsorption onto the EBMC for distilled water and SDBW. The equilibrium time adsorption capacities of the EBMC for the distilled water and the SDBW were calculated as 93.15 and 63.3 mg/g, respectively. There was a significant difference in the adsorption capacities between the distilled water and the SDBW. The results showed that the impurities in the SDBW occupied the adsorption sites of the EBMC. 70 min was used for the equilibrium time for further experiments. However, the equilibrium time was controlled under varying parameters such as pH, temperature, and the RB5 concentration and EBMC dosage.

Effect of pH

In this study, the effect of the pH (2, 3, 4, 5, 6, 7, 8, 9 and 10) on the adsorption of the RB5 onto the EBMC was performed at 20 °C with 250 mg/L initial dye concentration and a 0.1 g EBMC dosage. The pH value of the solution is one of the

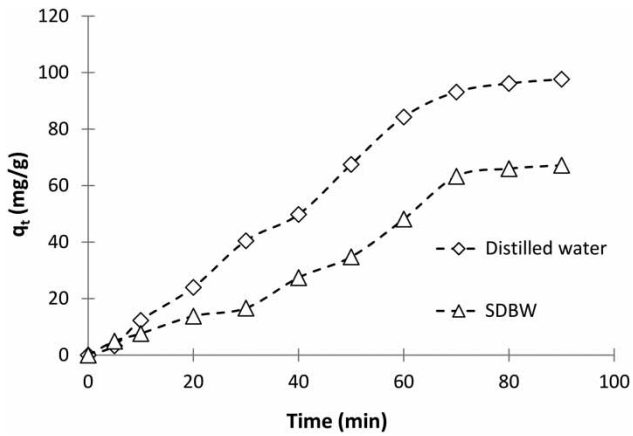


Figure 2 | Equilibriums for RB5 ($p \leq 0.05$).

Downloaded from https://iwaponline.com/wst/article-pdf/74/6/1386/458808/wst074061386.pdf
by guest

most important parameters that can alter the adsorption process. The pH value of the solution could change the charge density of the adsorbent surface, and the concentration of dissolved ions in the solution would affect the adsorption capacity of the adsorbent (Behzad *et al.* 2015). The effect of the pH on the adsorption of the RB5 onto the EBMC for the distilled water and SDBW is given in Figure 3. It was found that the pH has an important effect on the adsorption of RB5 onto EBMC. It was determined that 70 min is necessary to reach the equilibrium time for all the pH values. The adsorption capacity of the EBMC increased with the increasing pH. The adsorption capacities of the EBMC for the distilled water and SDBW within 70 min for the pH 2 were found to be 16.8 and 4.8 mg/g, respectively. It can be seen in Figure 3 that the adsorption capacity of the EBMC significantly increases above pH 7. The adsorption capacities of the EBMC for the distilled water and the SDBW within 70 min for the pH 10 were found to be 112.95 and 93.03 mg/g, respectively. The optimum pH for the adsorption of the RB5 onto the EBMC was found to be 10, and pH 10 was used for further experiments. At an acidic pH, values H^+ may occupy the adsorption sites of the EBMC. The low adsorption capacities at low pH values may occur due to the competitive adsorption between the H^+ ions and the RB5 molecules. The results showed that the H^+ ions inhibit the adsorption of the RB5 onto EBMC. The surface of the adsorbent may be charged negatively at high pH values, and the adsorption of the RB5 molecules increases due to the electrostatic attraction between the EBMC surface and the RB5 molecules. A similar result for the pH effect was also reported for the adsorption of methylene blue onto jute fiber carbon (Senthilkumaar *et al.* 2005).

Effect of temperature

The effect of the temperature (15, 20, 25, 30, 35, 40, 45, 50, and 50 °C) on the adsorption of the RB5 onto the EBMC was performed at pH 10 with a 250 mg/L initial dye concentration and 0.1 g EBMC dosage (Figure 4). Temperature is an important factor that indicates whether the adsorption process is exothermic or endothermic (Ghaedi *et al.* 2011). The adsorption capacity of the EBMC significantly increased with the increasing temperature, which indicates that the adsorption of the RB5 onto the EBMC was an endothermic process. The adsorption capacities of the EBMC for distilled water and SDBW within 70 min for 15 °C were found to be 94.80 and 76.65 mg/g, respectively. The adsorption capacities of the EBMC for distilled water and SDBW within 70 min for 55 °C were found to be 246.30 and 202.80 mg/g, respectively. It can be seen from Figure 4 that there were no significant differences between the adsorption capacities for 50 and 55 °C. Therefore, 50 °C was the selected optimum temperature for the adsorption of the RB5 by EBMC and 50 °C was used for further experiments. The higher adsorption capacities at higher temperatures may be due to the increasing mobility of the RB5 molecules. Also, the number of active sites of the EBMC may increase with the increasing temperature (Almeida *et al.* 2009; Sara & Tushar 2012).

Thermodynamic parameters

The thermodynamic parameters such as change in standard free energy (ΔG°), enthalpy (ΔH°), and entropy (ΔS°) were

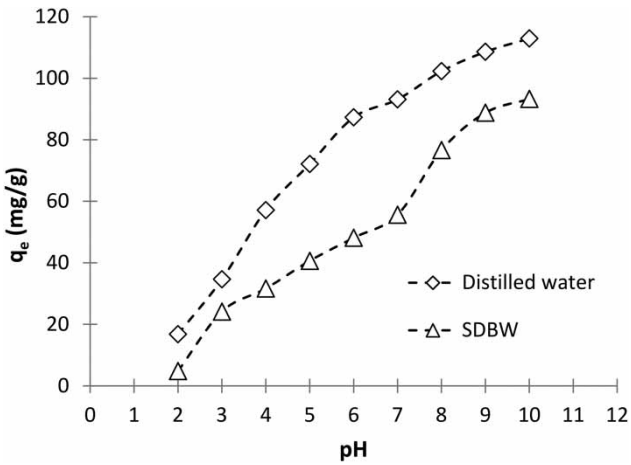


Figure 3 | The effect of pH on adsorption of RB5 onto EBMC for distilled water and SDBW ($p \leq 0.05$).

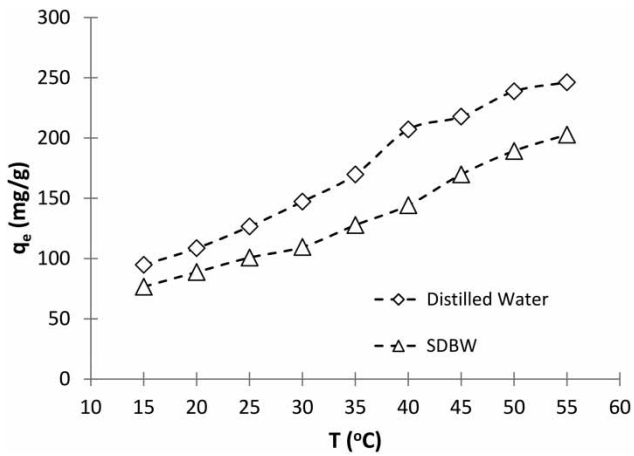


Figure 4 | Effect of temperature on the adsorption of RB5 onto EBMC for distilled water and SDBW ($p \leq 0.05$).

Downloaded from https://iwaponline.com/wst/article-pdf/74/6/1386/458808/wst074061386.pdf
by guest

Table 1 | Thermodynamic parameters of RB5 dye adsorption onto the EBMC at different temperatures

Temperature, °C	ΔG°, kJ/mol	ΔH°, kJ/mol	ΔS°, kJ/mol
15	2,471.264	36,571.04	118.402
20	1,879.254		
25	1,287.244		
30	695.234		
35	103.224		
40	−488.786		
45	−1,080.796		
50	−1,672.806		
55	−2,264.816		

estimated using the following equations:

$$\Delta G^{\circ} = \Delta H^{\circ} - T\Delta S^{\circ} \quad (11)$$

$$\log\left(\frac{q_e}{C_e}\right) = \frac{\Delta S^{\circ}}{2.303R} + \frac{-\Delta H^{\circ}}{2.303RT} \quad (12)$$

ΔH° and ΔS° were estimated from the slope and intercept of a graph plotting $\log(q_e/C_e)$ versus 1/T (figure not shown) where q_e is the amount of dye adsorbed per unit mass of the EBMC (mg/g) at the equilibrium, C_e is the equilibrium concentration (mg/L), T is temperature in K, and R is the gas constant (8.314 J/mol K) (Arias & Sen 2009).

The thermodynamic parameters were calculated in order to comprehend the feasibility and nature of the adsorption of the RB5 onto the EBMC for the distilled water. The results are presented in Table 1.

The negative ΔG° values were obtained over 35 °C. Therefore, the spontaneity of the RB5 adsorption onto the EBMC is favored at high temperatures. The positive values of ΔH° indicate the endothermic nature of the RB5 adsorption onto the EBMC. The positive value of ΔS° indicates that the degree of randomness at the solid–liquid interface increased during the RB5 dye adsorption onto the EBMC (Sara & Tushar 2012).

Effect of RB5 concentration

The effect of the initial RB5 concentration (75, 100, 150, 200 and 250 mg/L) on the adsorption of the RB5 onto the EBMC was performed while the temperature, the EBMC dosage, and the pH, were fixed at 50 mg/L, 0.1 g and 10, respectively. It was determined that the adsorption capacity of the EBMC significantly increased with the increasing initial concentration, and the RB5 removal efficiencies increased with the decreasing initial RB5 concentration. The effect of the initial RB5 concentration onto the adsorption capacity and removal efficiency is given in Figure 5. When the initial RB5 concentration increased from 75 mg/L to 250 mg/L, the adsorption capacity of the EBMC for the distilled water increased from 85.35 to 238.80 mg/g, while the removal percentage of the RB5 decreased from 75.86% to 63.68%. The adsorption capacity of the EBMC for the SDBW increased from 76.65 to 189.3 mg/g, while the removal percentage of the RB5 decreased from 68.13% to 50.48%.

Effect of the EBMC dosage

The investigation into the effects of the adsorbent dosage in the adsorption experiments is an important stage for

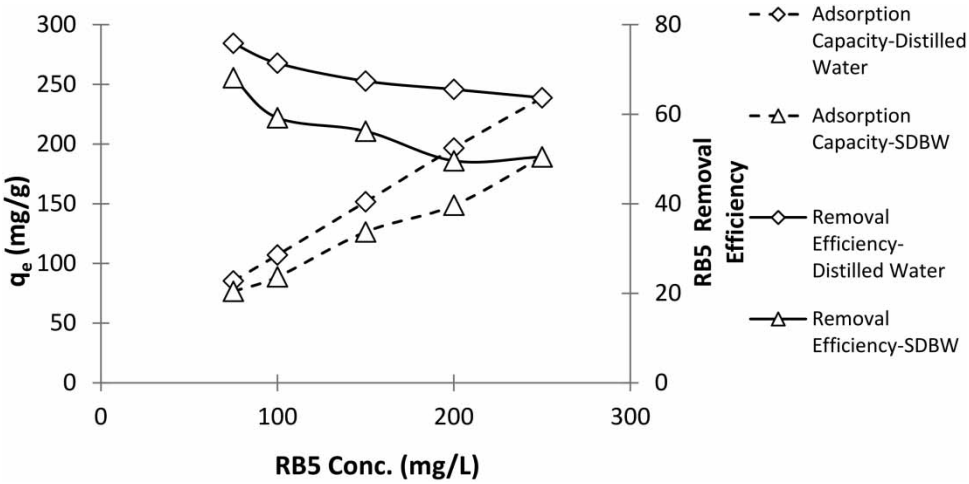


Figure 5 | Effect of initial RB5 concentration on adsorption capacity of EBMC and RB5 removal efficiency for distilled water and SDBW ($p \leq 0.05$).

Downloaded from https://iwaponline.com/wst/article-pdf/74/6/1386/458808/wst074061386.pdf
by guest

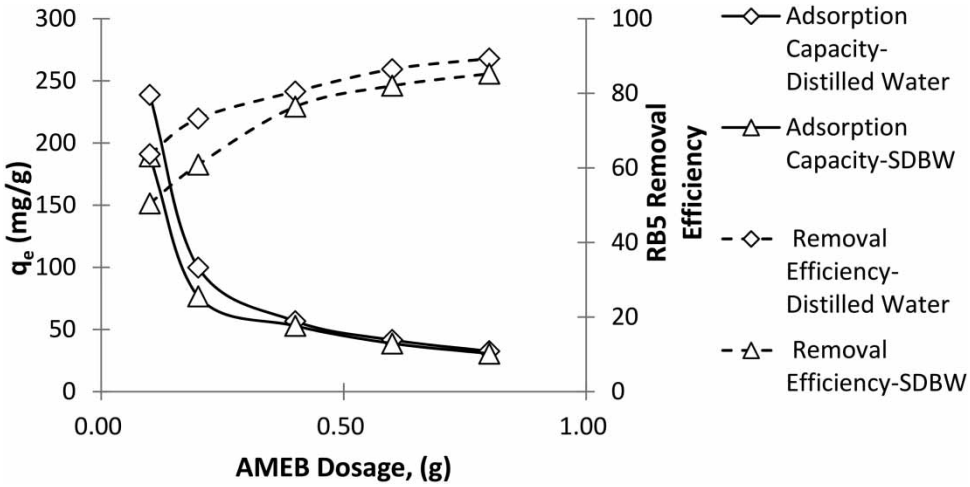


Figure 6 | Effect of EBMC dosage on the adsorption capacity of EBMC and RB5 removal efficiency for distilled water and SDBW ($p \leq 0.05$).

the determination of the adsorption capacity for the studied dye concentrations. The effect of the EBMC dosage (0.1, 0.2, 0.4, 0.6 and 0.8 g) on the adsorption of the RB5 onto the EBMC was performed while the initial dye concentration, temperature, and pH were fixed at 250 mg/L, 50 °C and 10, respectively. It was found from Figure 6 that the adsorption capacity of the EBMC for the distilled water significantly increased from 32.48 to 238.80 mg/g with the decrease of the adsorbent dosage from 0.8 g to 0.1 g. The increase in the adsorption capacity with the decreasing EBMC dosage is due to the concentration gradient between the RB5 concentration in the solution and in the surface of the EBMC (Sara & Tushar 2012). This may be explained by the increase in the availability of the surface active sites with the increasing doses of the EBMC (Kannan & Sundaram 2001). It was also found that the percentage of dye removal for the distilled water increased from 63.68% to 89.32% with the increase of the adsorbent mass from 0.1 g to 0.8 g. The dye removal efficiency for the SDBW increased from 50.48% to 85.28% with the increase of the adsorbent mass from 0.1 g to 0.8 g. 0.6 g EBMC was found to be sufficient to remove 250 mg/L RB5 from 150 mL of distilled water with ~85% removal efficiency. However, over 0.8 g EBMC was required to obtain 85% removal efficiency for SDBW.

Equilibrium isotherms

The data were used from the section 'Effect of RB5 concentration' to calculate the isotherm parameters for the distilled water. The estimated isotherm parameters are given in Table 2.

A 370.7 mg/g maximum adsorption capacity of the EBMC was obtained from the Langmuir isotherm with a 0.983 correlation coefficient and a 2.121% APE. D-R and Jovanovic isotherms predicted the maximum adsorption capacity of 264.8 and 288.9 mg/g, respectively. However, low correlation coefficients and high APEs were obtained from these isotherms. Therefore, a 370.7 mg/g adsorption capacity, which was predicted from the Langmuir isotherm, was selected as the maximum adsorption capacity of the EBMC for the RB5. According to Table 2, the coefficient

Table 2 | Model parameters estimated for the adsorption isotherms RB5 by EBMC (pH = 7, T = 20 °C, particle size = 1 mm, EBMC dosage = 0.5 g)

Isotherms	Parameters		APE, %
Langmuir	q_{max}	370.7	2.121
	K_L	6.310	
	R^2	0.983	
Freundlich	1/n	0.563	0.771
	K_F	18.26	
	R^2	0.989	
D-R	q_{max}	264.8	2.687
	B_D	0.00731	
	R^2	0.863	
Jovanovic	q_{max}	288.9	3.55
	K_J	−0.022	
	R^2	0.931	
Koble–Corrigan	a	25.81	0.557
	n	0.245	
	b	−0.221	
	R^2	0.997	

Downloaded from https://iwaponline.com/wst/article-pdf/74/6/1386/458808/wst074061386.pdf
by guest

Table 3 | Adsorption capacities of various alternative adsorbents for RB5

Adsorbent	Isotherm	Adsorbent capacity, mg/g	Reference
EBMC	Langmuir	370.7	Present study
Modified sepiolite	Langmuir	120.50	Orhan *et al.* (2004)
Modified zeolite	Langmuir	60.5	Orhan *et al.* (2004)
Activated sludge	Langmuir	116	Gulnaz *et al.* (2006)
Schizophyllum commune	Langmuir	180.17	Renganathan *et al.* (2006)
Chitin	Langmuir	130	Urszula (2007)
Chitosan flakes	Langmuir	480	Urszula (2007)
Chitosan beads	Langmuir	400	Urszula (2007)
Aspergillus foetidus	Langmuir	106	Rachna & Sumathi (2008)
Surfactant-modified activated carbon	Langmuir	100	Choi *et al.* (2008)
Furnace slag	Langmuir	74.4	Xue *et al.* (2009)
Cetyltrimethylammonium bromide-coated magnetite	Langmuir	312.5	Faraji *et al.* (2010)
Peanut hull	Langmuir	55.5	Saban Tanyildizi (2011)
Orange peel	Langmuir	62.6	Elsa *et al.* (2012)
Ionic liquid grafted-magnetic nanoparticles	Langmuir	161.29	Poursaberi & Hassanisadi (2013)
Scallop shell	Langmuir	90.9	Shirzad-Siboni *et al.* (2014)
Pumice	Langmuir	12.85	Behzad *et al.* (2014)
AC from walnut wood	Langmuir	19.34	Behzad *et al.* (2014)
$ZnO–Fe_3O_4$	Langmuir	22.1	Mehrdad *et al.* (2014)
Bentonite clay	Langmuir	34	Muhammad *et al.* (2015)
Chitosan-intercalated montmorillonite	Langmuir	138.89	Chakkrit & Songsak (2015)
Silica–alumina oxide	Langmuir	47.10	Monika *et al.* (2015)
Polyaniline coated ingo-cellulose	Langmuir	312	Niladri *et al.* (2015)
Carob processing waste	Langmuir	36.90	Fuat *et al.* (2015)
F_30_4-based char	Langmuir	2.88	Ayesha *et al.* (2015)
$Cu–Cu_2O$-based char	Langmuir	6.06	Ayesha *et al.* (2015)
Polyaniline nanofibers	Langmuir	434.7	Madhumita *et al.* (2016)
Aspergillus versicolor biomass	Langmuir	227.27	Jian *et al.* (2016)

of the correlation (0.989) of the Freundlich model is better than the Langmuir. The mean value of the APE of the Freundlich isotherm was calculated at 0.771%. The value of 1/n (0.563) indicated favorable adsorption and intensity of the surface heterogeneity. The highest correlation coefficient (0.997) and lowest APE (0.557) were obtained from the Koble–Corrigan isotherm. Therefore, the Koble–Corrigan isotherm described the adsorption process better than the Langmuir, Freundlich, D-R, and Jovanovic isotherm models.

The comparison of the adsorption capacities of the different low cost adsorbents for the RB5 under similar experimental conditions is given in Table 3. It shows that the EBMC has a large adsorption capacity when compared to many other low-cost adsorbents. The adsorption capacity of the chitosan flakes, the chitosan beads, and the polyaniline nanofibers, have higher adsorption capacities than the EBMC. On the other hand, *Eucalyptus camaldulensis* bark possesses a low-cost adsorbent due to its renewable character, wide availability and accessibility.

MLR analyses

The MLR analysis was performed in order to model the effects of the experimental conditions such as the contact time, the pH, temperature, the initial BPA concentration, and the EBMC dosage on the q_e values. The coefficients of

Downloaded from https://iwaponline.com/wst/article-pdf/74/6/1386/458808/wst074061386.pdf
by guest

Table 4 | Coefficients of MLR model for Aqueous Solution and SDBW

Model		Unstandardized coefficients B	Standardized coefficients Std error	Beta	t	Sig.
Constant	Aqueous S.	−275.454	20.27		−13.58	0.000
	SDBW	−240.968	15.757		−15.293	0.000
Contact time	Aqueous S.	1.237	0.13	0.32	9.20	0.000
	SDBW	1.012	0.102	0.329	9.955	0.000
pH	Aqueous S.	10.987	1.30	0.36	8.44	0.000
	SDBW	11.032	1.090	0.373	10.125	0.000
Temperature	Aqueous S.	3.164	0.25	0.65	12.56	0.000
	SDBW	2.746	0.181	0.705	15.152	0.000
Initial BPA conc.	Aqueous S.	0.676	0.064	0.40	10.54	0.000
	SDBW	0.505	0.048	0.379	10.425	0.000
EBMC dosage	Aqueous S.	−332.241	17.547	−0.724	−18.934	0.000
	SDBW	−244.156	13.269	−0.659	−18.400	0.000
R^2 for q_e (exp) and q_e (pred.)	Aqueous S.		0.893			
	SDBW		0.906			

the MLR models for the aqueous solution and the SDBW are given in Table 4. The models obtained from the MLR analysis for the aqueous solution and the SDBW are given in Equations (13) and (14), respectively.

$$q_{e_{pred}} = -275.454 + 1.237X_1 + 10.987X_2 + 3.164X_3 + 0.676X_4 - 332.241X_5 \quad (13)$$

$$q_{e_{pred}} = -240.968 + 1.012X_1 + 11.032X_2 + 32.746X_3 + 0.505X_4 - 244.156X_5 \quad (14)$$

where X_1 is the contact time, X_2 is the pH value, X_3 is the temperature, X_4 is the BPA concentration, and X_5 is the dosage of the EBMC.

It can be seen from Table 4 that the EBMC dosage is the most effective parameter on the adsorption capacity at the equilibrium due to the highest coefficients for the aqueous solution and SDBW. The negative value showed the negative relationship between the adsorption capacity and the EBMC dosage. It was mentioned above that the increase in the adsorption capacity with the decreasing EBMC dosage is due to the concentration gradient between the RB5 concentration in the solution and in the surface of the EBMC (Sara & Tushar 2012). The correlation coefficients for the experimental q_e and the MLR predicted q_e was calculated as 0.893 for the aqueous solution (figure not shown). According to the MLR, the independent variables accounted for 89.3% of the total variability of q_e for the aqueous solution. Also, the independent variables accounted for 90.6% of the total variability of the q_e for the SDBW.

Cost analysis

The maximum adsorption capacity of an adsorbent for textile dye is the most important parameter. However, the maximum adsorption capacity is not sufficient to evaluate the potential use of the adsorbents. Although the literature rarely reports the cost analysis of the tested adsorbents, it is important to evaluate the potential use of the adsorbents in the industrial processes. In this study, *E. camaldulensis* barks were selected as a low-cost adsorbent due to their renewable character and wide availability. Eucalyptus is known worldwide as a source of fiber for the pulp and paper industry (Marília *et al.* 2014). Moreover, the abundant amounts of barks are produced during the debarking process. A simple cost estimation was performed for the production and use of EBMC. Approximately $200 was calculated for the production of one ton of the EBMC after considering the cost of transport, chemicals, and electrical energy. The price of the commercially activated carbon, ranging from $700 to $5,000/ton, depends on the quality (Saygili *et al.* 2015). Thus, the price of the EBMC is significantly cheaper than the commercially activated carbon. Furthermore, as a result of the experiments, an approximate $0.035 cost was calculated for the complete removal of 10 mg/L of the RB5 from 1 m^3 textile wastewater by the EBMC.

Downloaded from https://iwaponline.com/wst/article-pdf/74/6/1386/458808/wst074061386.pdf
by guest

CONCLUSION

The experiments showed that the EBMC removed the RB5 successfully from the distilled water and the SDBW. The adsorption capacities of the EBMC and the RB5 removal efficiencies for the distilled water were found to be higher than for the SDBW. The results of the present study showed that EBMC can be used as an alternative low-cost adsorbent for the effective removal of RB5, which is a diazo textile dye. The adsorption capacity of the EBMC was found to increase by increasing initial dye concentrations, temperature, and pH, and was found to increase with decreasing dosage of EBMC. 0.6 g EBMC was found to be sufficient to remove 250 mg/L RB5 from 150 mL distilled water with ~85% removal efficiency. On the other hand, 0.8 g EBMC was found to be sufficient to remove 250 mg/L RB5 from 150 mL SDBW with ~85% removal efficiency. The Langmuir isotherm predicted a 370.7 mg/g maximum adsorption capacity of EBMC for the RB5 with a 0.983 correlation coefficient. The value of 1/n (0.563) obtained from the Freundlich isotherm indicated favorable adsorption and intensity of the surface heterogeneity. The Koble–Corrigan isotherm described the adsorption process better than the Langmuir, Freundlich, D-R and Jovanovic isotherm models with a 0.997 correlation coefficient and 0.557 APE. The thermodynamic analysis showed that the adsorption of the RB5 onto the EBMC was an endothermic process. The MLR analysis showed that the dosage of the EBMC is the most effective parameter on the adsorption capacity at the equilibrium.

ACKNOWLEDGEMENTS

The authors would like to thank Cukurova University for their support.

REFERENCES

Allen, S. J., Gan, Q., Matthews, R. & Johnson, P. A. 2003 Comparison of optimised isotherm models for basic dye adsorption by kuzdu. *Bioresource Technology* **88**, 143–152.

Almeida, C. A. P., Debacher, N. A., Downs, A. J., Cottet, L. & Mello, C. A. D. 2009 Removal of methylene blue from colored effluents by adsorption on montmorillonite clay. *Journal of Colloid and Interface Science* **332**, 46–53.

Arias, F. & Sen, T. K. 2009 Removal of zinc metal ion (Zn^{2+}) from its aqueous solution by kaolin clay mineral: a kinetic and equilibrium study. *Colloids and Surfaces* **348**, 100–108.

Ayesha, K., Audil, R. & Rafia, Y. 2015 Adsorption of Reactive Black-5 by pine needles biochar produced via catalytic and non-catalytic pyrolysis. *Arabian Journal for Science and Engineering* **40**, 1269–1278.

Behzad, H., Susana, R., Abdeltif, A., Mohd, R., Alaa, H. & Mohammad, A. A. 2014 Uptake of Reactive Black 5 by pumice and walnut activated carbon: Chemistry and adsorption mechanisms. *Journal of Industrial and Engineering Chemistry* **20**, 2939–2947.

Behzad, H., Susana, R. C., Mohammad, A. A., Mohammad, A., Inderjeet, T., Shilpi, A. & Vinod Kumar, G. 2015 Kinetics and thermodynamics of enhanced adsorption of the dye AR 18 using activated carbons prepared from walnut and poplar woods. *Journal of Molecular Liquids* **208**, 99–105.

Bennani, A. K., Mounir, B., Hachkar, M., Bakassec, M. & Yaacoubi, A. 2009 Removal of Basic Red 46 dye from aqueous solution by adsorption onto Moroccan clay. *Journal of Hazardous Materials* **168**, 304–309.

Chakkrit, U. & Songsak, S. 2015 Adsorption characteristics of reactive black 5 onto chitosan-intercalated montmorillonite. *Desalination and Water Treatment* **53**, 2962–2969.

Chan, L. S., Cheung, W. H., Allen, S. J. & McKay, G. 2012 Error analysis of adsorption isotherm models for acid dyes onto bamboo derived activated carbon. *Chinese Journal of Chemical Engineering* **20** (3), 535–542.

Choi, H. D., Shin, M. C., Kim, D. H., Jeon, C. S. & Baek, K. 2008 Removal characteristics of reactive black 5 using surfactant-modified activated carbon. *Desalination* **223**, 290–298.

Contreras, E. G., Martinez, B. E., Sepulveda, L. A. & Palma, C. L. 2008 Palma kinetics of basic dye adsorption onto Sphagnum Magellanicum Peat. *Adsorption Science and Technology* **25** (9), 637–645.

Contreras, E., Sepulveda, L. & Palma, C. 2012 Valorization of agroindustrial wastes as biosorbent for the removal of textile dyes from aqueous solutions. *International Journal of Chemical Engineering* **2012**, 1–9.

Crawford, H. B. & Gretlyn, C. 1990 *Water Treatment Plant Design*. 2nd edn. American Society of Civil Engineers/American Water Works Association, McGraw-Hill, New York.

Dabrowski, A. 2001 Adsorption from theory to practice. *Advances in Colloid and Interface Science* **93** (1–3), 135–224.

Dawood, S. & Sen, T. K. 2012 Removal of anionic dye Congo red from aqueous solution by raw pine and acid-treated pine cone powder as adsorbent: equilibrium, thermodynamic, kinetics, mechanism and process design. *Water Research* **46**, 1933–1946.

Faraji, M., Yamini, Y., Tahmasebi, E., Saleh, A. & Nourmohammadian, F. 2010 Cetyltrimethylammonium bromide-coated magnetite nanoparticles as highly efficient adsorbent for rapid removal of reactive dyes from the textile companies wastewaters. *Journal of the Iranian Chemical Society* **7**, 130–144.

Foo, K. Y. & Hameed, B. H. 2010 Insights into the modeling of adsorption isotherm systems. *Chemical Engineering Journal* **156** (1), 2–10.

Freundlich, H. M. F. 1906 Over the adsorption in solution. *Journal of Physical Chemistry* **57**, 385–470.

Downloaded from https://iwaponline.com/wst/article-pdf/74/6/1386/458808/wst074061386.pdf
by guest

Fuat, G., Hasan, S., Gülbahar, A. S. & Filiz, K. 2015 New low-cost nanoporous carbonaceous adsorbent developed from carob (*Ceratonia siliqua*) processing industry waste for the adsorption of anionic textile dye: characterization, equilibrium and kinetic modeling. *Journal of Molecular Liquids* **206**, 244–255.

Gabriela, G. S., Selene, M. A., Guelli, U. S., Debora, O. & Antonio, A. U. S. 2016 The application of textile sludge adsorbents for the removal of Reactive Red 2 dye. *Journal of Environmental Management* **168**, 149–156.

Ghaedi, M., Hassanzadeh, A. & NasiriKokhdan, S. 2011 Multiwalled carbon nanotubes as adsorbents for the kinetic and equilibrium study of the removal of alizarin red S and Morin. *Journal of Chemical & Engineering Data* **56**, 2511–2520.

Gulnaz, O., Kaya, A. & Dincer, S. 2006 The reuse of dried activated sludge for adsorption of reactive dye. *Journal of Hazardous Materials* **134**, 190–196.

Ilda, V., Yasemin, K. A., Unal, S. E., Zeren, B. G. & Coskun, A. 2012 Techno-economic analysis of textile dye bath wastewater treatment by integrated membrane processes under the zero liquid discharge approach. *Resources, Conservation and Recycling* **58**, 25–35.

Ipek, G., Gulerman, A. S. & Filiz, B. D. 2006 Importance of H_2O_2/Fe^{2+} ratio in Fenton's treatment of a carpet dyeing wastewater. *Journal of Hazardous Materials* **136**, 763–769.

Jian, H., Dongfang, L., Jianbo, L., Hao, W., Xiaocheng, W. & Jinzhe, L. 2016 Biosorption of reactive black 5 by modified *Aspergillus versicolor* biomass: kinetics, capacity and mechanism studies. *Colloids and Surfaces A: Physicochem. Eng. Aspects* **492**, 242–248.

Kannan, N. & Sundaram, M. M. 2001 Kinetics and mechanism of removal of methylene blue by adsorption on various carbons – a comparative study. *Dyes and Pigments* **51**, 25–40.

Kouassi, N. A., Yao, A. Y., Kouassi, B. Y., Droh, L. G. & Albert, T. 2015 Investigation of dye adsorption onto activated carbon from the shells of Macoré fruit. *Journal of Environmental Management* **156**, 10–14.

Kumar, P., Agnihotri, R., Wasewar, K. L., Uslu, H. & Yoo, C. K. 2012 Status of adsorptive removal of dye from textile industry effluent. *Desalination and Water Treatment* **50**, 226–244.

Langmuir, I. 1918 Adsorption of gases on plain surfaces of glass mica platinum. *Journal of the American Chemical Society* **40**, 136–403.

Little, E. L. 1983 *Common Fuelwood Crops: A Handbook for their Identification*. McClain Printing Co., Parsons, WV, USA.

Luiz, C. A. O., Diego, I. P., Alessandra, S. & Sibele, B. C. P. 2004 Magnetic zeolites: a new adsorbent for removal of metallic contaminants from water. *Water Research* **38**, 3699–3704.

Madhumita, B., Rob, I. M., Arjun, M., Shilpi, A. & Vinod, K. G. 2016 Polyaniline nanofibers as highly effective re-usable adsorbent for removal of reactive black 5 from aqueous solutions. *Journal of Colloid and Interface Science* **466**, 442–451.

Malik, P. K. 2003 Use of activated carbons prepared from saw dust and rice-husk for adsorption of acid dyes: a case study of Acid Yellow 36. *Dyes and Pigments* **56**, 239–249.

Marília, P., Doahn, F., Vicelina, B. S., Teresa, Q., Sofia, K. & Helena, P. 2014 Evaluation on paper making potential of nine *Eucalyptus* species based on wood anatomical features. *Industrial Crops and Products* **54**, 327–334.

Mehrdad, F., Seyydeh, H., Jae-Kyu, Y. & Mehdi, S. 2014 Application of ZnO–Fe_3O_4 nanocomposite on the removal of azo dye from aqueous solutions: kinetics and equilibrium studies. *Water, Air & Soil Pollution* **225**, 2–12.

Mohammad, R. S., Mahdi, H. & Gordon, M. 2014 Breakthrough curve analysis for fixed-bed adsorption of azo dyes using novel pine cone–derived active carbon. *Adsorption Science and Technology* **32** (10), 791–806.

Mohan, D., Singh, K. P., Singh, G. & Kumar, K. 2002 Removal of dyes from wastewater using flyash, a low-cost adsorbent. *Industrial & Engineering Chemistry Research* **41**, 3688–3695.

Monika, W., Małgorzata, W., Vladimir, M. G. & Vladimir, I. Z. 2015 Adsorptive removal of acid, reactive and direct dyes from aqueous solutions and wastewater using mixed silica–alumina oxide. *Powder Technology* **278**, 306–315.

Muhammad, T. A., Abdulrahman, A. A. & Muhammad, S. 2015 Adsorptive removal of reactive Black 5 from wastewater using bentonite clay: isotherms, kinetics and thermodynamics. *Sustainability* **7**, 15302–15318.

Myslak, Z. W. & Bolt, H. M. 1988 Occupational Exposure to azo dyes and risk of bladder cancer. *Zbl. Arbeitsmed* **38**, 310–321.

Nethaji, S., Sivasamy, A. & Mandal, A. B. 2013 Preparation and characterization of corn cob activated carbon coated with nano-sized magnetite particles for the removal of Cr(VI). *Bioresource Technology* **134**, 94–100.

Nevine, K. A. 2008 Removal of reactive dye from aqueous solutions by adsorption onto activated carbons prepared from sugarcane bagasse pith. *Desalination* **223**, 152–161.

Niladri, B., Sushanta, D., Kriveshini, P. & Arjun, M. 2015 Efficient removal of Reactive Black from aqueous solution using polyaniline coated ligno-cellulose composite as a potential adsorbent. *Journal of Molecular Liquids* **209**, 387–396.

Orhan, O., Bulent, A., Mustafa, T. & Mehmet, S. C. 2004 Comparison of the adsorption characteristics of azo-reactive dyes on mezoporous minerals. *Dyes and Pigments* **62**, 49–60.

Poursaberi, T. & Hassanisadi, M. 2013 Magnetic removal of reactive black 5 from wastewater using ionic liquid grafted-magnetic nanoparticles. *Clean – Soil, Air, Water* **41** (12), 1208–1215.

Rachna, P. & Sumathi, S. 2008 Kinetic and equilibrium studies on the biosorption of reactive black 5 dye by Aspergillus foetidus. *Bioresource Technology* **99**, 51–58.

Rafael, C., Luis, A., Renata, C., Luis, H. & Valeria, P. 2013 Adsorption isotherms and thermodynamics of α-lactalbumin on an anionic exchanger. *Fluid Phase Equilibria* **348**, 39–44.

Renganathan, S., Richard, T. W., Lima, R. M., Gautam, P. & Velan, M. 2006 Accumulation of Acid Orange 7, Acid Red 18 and Reactive Black 5 by growing Schizophyllum commune. *Bioresource Technology* **97**, 2189–2193.

Saban Tanyildizi, M. 2011 Modeling of adsorption isotherms and kinetics of reactive dye from aqueous solution by peanut hull. *Chemical Engineering Journal* **168**, 1234–1240.

Downloaded from https://iwaponline.com/wst/article-pdf/74/6/1386/458808/wst074061386.pdf
by guest

Saygili, H., Guzel, F. & Onal, Y. 2015 Conversion of grape industrial processing waste to activated carbon sorbent and its performance in cationic and anionic dyes adsorption. *Journal of Cleaner Production* **93**, 84–93.

Senthilkumaar, S., Varadarajan, P. R., Porkodi, K. & Subbhuraam, C. V. 2005 Adsorption of methylene blue onto jute fiber carbon: kinetics and equilibrium studies. *Journal of Colloid and Interface Science* **284**, 78–82.

Senthil Kumar, P., Ramakrishnan, K., Dinesh Kirupha, S. & Sivanesan, S. 2010 Thermodynamic and kinetic studies of cadmium adsorption from aqueous solution onto rice husk. *Brazilian Journal of Chemical Engineering* **27** (2), 347–355.

Shirzad-Siboni, M., Khataee, A. & Joo, S. W. 2014 Kinetics and equilibrium studies of removal of an azo dye from aqueous solution by adsorption onto scallop. *Journal of Industrial and Engineering Chemistry* **20**, 610–615.

Subramanyam, B. & Ashutosh, D. 2012 Adsorption isotherm modeling of phenol onto natural soils – applicability of various isotherm models. *International Journal of Environmental Research and Public Health* **6** (1), 265–276.

Suhong, C., Jian, Z., Chenglu, Z., Qinyan, Y., Yan, L. & Chao, L. 2010 Equilibrium and kinetic studies of methylorange and methylviolet adsorption on activated carbon derived from *Phragmitesaustralis*. *Desalination* **252**, 149–156.

Taimur, K., Shamsul, R. M. K. & Malay, C. 2010 Adsorptive removal of reactive Yellow 15 from aqueous solution by coconut coir activated carbon. *Adsorption Science and Technology* **28** (7), 657–667.

Urszula, F. 2007 Adsorption and desorption of reactive dyes onto chitin and chitosan flakes and beads. *Adsorption Science and Technology* **24** (9), 781–796.

Utkan, O., Bilge, O., Sevil, V. & Sibel, Z. 2011 Modeling adsorption of sodium dodecyl benzene sulfonate (SDBS) onto polyaniline (PANI) by using multi linear regression and artificial neural networks. *Chemical Engineering Journal* **178**, 183–190.

Walker, G. M. & Weatherley, L. R. 1997 Adsorption of acid dyes onto granular activated carbon in fixed beds. *Water Research* **31** (8), 2093–2101.

Wang, L. 2012 Application of activated carbon derived from 'waste' bamboo culms for the adsorption of azo disperse dye: kinetic, equilibrium and thermodynamic studies. *Journal of Environmental Management* **102**, 79–82.

Weber, T. W. & Chakkravorti, R. K. 1974 Pore and solid diffusion models for fixed bed adsorbers. *AICHE Journal* **20** (2), 228–238.

Wong, Y. C., Szeto, Y. S., Cheung, W. H. & McKay, G. 2004 Adsorption of acid dyes on chitosan– equilibrium isotherm analyses. *Process Biochemistry* **39** (6), 695–704.

Xue, Y., Hou, H. & Zhu, S. 2009 Adsorption removal of reactive dyes from aqueous solution by modified basic oxygen furnace slag: isotherm and kinetic study. *Chemical Engineering Journal* **147**, 272–279.

Yadav, K. R., Sharma, R. K. & Kothari, R. M. 2002 Bioconversion of eucalyptus bark waste into soil conditioner. *Bioresource Technology* **81** (2), 163–165.

First received 8 February 2016; accepted in revised form 13 June 2016. Available online 27 June 2016

Downloaded from https://iwaponline.com/wst/article-pdf/74/6/1386/458808/wst074061386.pdf
by guest